The EMBO Journal Vol. 19 No. 9 pp. 2069–2081, 2000

Targeted disruption of *Skp2* results in accumulation of cyclin E and p27^{Kip1}, polyploidy and centrosome overduplication

Keiko Nakayama[1,2], Hiroyasu Nagahama[2,3], Yohji A.Minamishima[2,3], Masaki Matsumoto[2,3], Ikuo Nakamichi[2,3], Kyoko Kitagawa[3], Michiko Shirane[2,3], Ryosuke Tsunematsu[2,3], Tadasuke Tsukiyama[2,3], Noriko Ishida[2,3], Masatoshi Kitagawa[2,3], Kei-ichi Nakayama[1,2,3,4] and Shigetsugu Hatakeyama[2,3]

[1]Laboratory of Embryonic and Genetic Engineering and [3]Department of Molecular and Cellular Biology, Medical Institute of Bioregulation, Kyushu University, 3-1-1 Maidashi, Higashi-ku, Fukuoka 812-8582 and [2]CREST, Japan Science and Technology Corporation (JST), 4-1-8 Honcho, Kawaguchi, Saitama 332-0012, Japan

[4]Corresponding author
e-mail: nakayak1@bioreg.kyushu-u.ac.jp

The ubiquitin–proteasome pathway plays an important role in control of the abundance of cell cycle regulators. Mice lacking Skp2, an F-box protein and substrate recognition component of an Skp1–Cullin–F-box protein (SCF) ubiquitin ligase, were generated. Although *Skp2*$^{-/-}$ animals are viable, cells in the mutant mice contain markedly enlarged nuclei with polyploidy and multiple centrosomes, and show a reduced growth rate and increased apoptosis. *Skp2*$^{-/-}$ cells also exhibit increased accumulation of both cyclin E and p27^{Kip1}. The elimination of cyclin E during S and G_2 phases is impaired in *Skp2*$^{-/-}$ cells, resulting in loss of cyclin E periodicity. Biochemical studies showed that Skp2 interacts specifically with cyclin E and thereby promotes its ubiquitylation and degradation both *in vivo* and *in vitro*. These results suggest that specific degradation of cyclin E and p27^{Kip1} is mediated by the SCF^{Skp2} ubiquitin ligase complex, and that Skp2 may control chromosome replication and centrosome duplication by determining the abundance of cell cycle regulators.

Keywords: cyclin E/F-box protein/SCF complex/Skp2/ubiquitin ligase

Introduction

The ubiquitin–proteasome pathway of protein degradation plays an important role in control of the abundance of short-lived regulatory proteins (reviewed by Weissman, 1997; Hershko and Ciechanover, 1998). The rapidity and substrate specificity of protein degradation by the ubiquitin–proteasome pathway are consistent with its role in controlling the fluctuations in the intracellular concentrations of cyclins (King *et al*., 1995; Sudakin *et al*., 1995; Clurman *et al*., 1996; Won and Reed, 1996) and cyclin-dependent kinase (CDK) inhibitors (CKIs), such as p27^{Kip1} (Pagano *et al*., 1995).

The ubiquitin-mediated pathway of protein degradation comprises two discrete steps: the covalent attachment of multiple ubiquitin molecules to the protein substrate, and degradation of the polyubiquitylated protein by the 26S proteasome complex. The ubiquitin attachment system consists of several components that act in concert (Hershko *et al*., 1983; Scheffner *et al*., 1995). A ubiquitin-activating enzyme (E1) uses ATP to form a thioester bond between itself and ubiquitin, and it then transfers the activated ubiquitin to a ubiquitin-conjugating enzyme (E2). Certain E2 enzymes transfer ubiquitin directly to the protein substrate, whereas others require the participation of a third component, termed ubiquitin ligase (E3). Although the E3 components are thought to be primarily responsible for substrate recognition, they are the least well understood of the enzymes of the ubiquitin conjugation system.

Two major classes of ubiquitin ligase, which determine the specificity in protein ubiquitylation, are thought to regulate cell cycle progression: the SCF complex is implicated in G_1–S progression, and the anaphase-promoting complex or cyclosome (APC/C) is necessary for separation of sister chromatids at anaphase and for exit from M phase into G_1 (reviewed by Zachariae and Nathmyth, 1999). The SCF complexes consist of the invariable components Skp1, Cul1 and Rbx1/ROC1, as well as a variable component, known as an F-box protein, that binds to Skp1 through its F-box motif and serves as the substrate recognition subunit (Bai *et al*., 1996; Feldman *et al*., 1997; Skowyra *et al*., 1997). Skp2, which contains an F-box domain followed by leucine-rich repeats, was identified originally as a protein that interacts with the cyclin A–CDK2 complex (Zhang *et al*., 1995). Recently, however, biochemical data have implicated Skp2 in the ubiquitin-mediated degradation of p27^{Kip1} (Carrano *et al*., 1999; Tsvetkov *et al*., 1999) and the transcription factor E2F-1 (Marti *et al*., 1999). Skp2 begins to accumulate at late G_1 and its abundance is maximal during S and G_2 phases (Zhang *et al*., 1995; Carrano *et al*., 1999; Marti *et al*., 1999).

With the use of gene targeting in embryonic stem (ES) cells, we have now generated mice lacking Skp2. Cells derived from these animals exhibit hyperaccumulation of both cyclin E and p27^{Kip1}, polyploidy and multiple centrosomes. Consistent with these observations, our biochemical analysis indicates that Skp2 mediates ubiquitin-dependent degradation of cyclin E. Taken together, these data suggest that SCF^{Skp2} functions as the principal ubiquitin ligase in determining the abundance of cell cycle regulatory proteins at the G_1–S transition, thereby ensuring strict control of chromosomal replication and centrosome duplication.

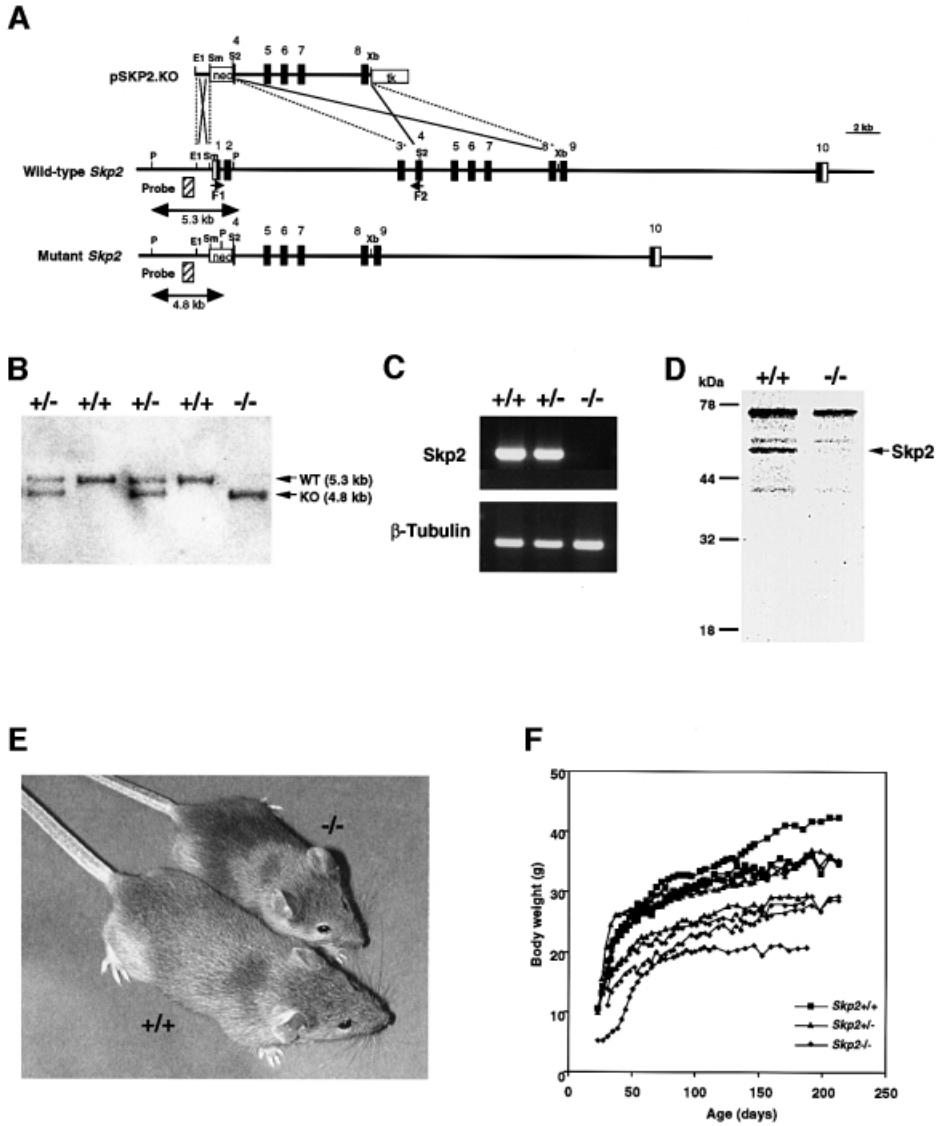

Fig. 1. Targeted disruption of mouse *Skp2*. (**A**) Structures of the targeting vector (pSKP2.KO), of the mouse *Skp2* locus and of the mutant allele resulting from homologous recombination. The coding exons or portions of exons are depicted by filled boxes, and the open boxes denote the non-coding portions. A genomic fragment used as a probe for Southern blot analysis is shown as a striped box, and the expected sizes of the *Pst*I fragments that hybridize with the probe are indicated. The positions of a set of primers (F1 and F2) used for RT–PCR analysis are also indicated. neo, the neomycin transferase gene linked to the PGK promoter; tk, thymidine kinase gene derived from herpes simplex virus linked to the PGK promoter. The orientations of both neo and tk were the same as that of *Skp2*. Restriction sites: E1, *Eco*RI; P, *Pst*I; S2, *Sac*II; Sm, *Sma*I; Xb, *Xba*I. Not all restriction sites are shown. (**B**) Southern blot analysis of genomic DNA extracted from mouse tails. The DNA was digested with *Pst*I and subjected to hybridization with the probe shown in (A). (**C**) RT–PCR analysis of *Skp2* (upper panel) or the β-tubulin gene (lower panel) in $Skp2^{+/+}$, $Skp2^{+/-}$ and $Skp2^{-/-}$ MEFs. (**D**) Immunoprecipitation analysis of radiolabeled Skp2 protein in $Skp2^{+/+}$ and $Skp2^{-/-}$ MEFs. The position of Skp2 is indicated on the right. (**E**) Representative male $Skp2^{+/+}$ and $Skp2^{-/-}$ littermates at 4 weeks of age. (**F**) Representative growth curves of male $Skp2^{+/+}$, $Skp2^{+/-}$ and $Skp2^{-/-}$ mice. Similar differences in body weight were apparent among female mice of the three genotypes (data not shown).

Results

Generation of Skp2 $^{-/-}$ mice

The mouse *Skp2* genomic locus comprises at least 10 exons spanning ~36 kb. The targeting construct was designed to delete the region from the translation initiation site to the site corresponding to the C-terminus of the F-box domain (Figure 1A). ES cells were transfected with the linearized targeting vector and recombinant clones were selected. Recombinant ES clones were injected into C57BL/6 blastocysts, and chimeric males that transmitted the mutant allele to the germline were obtained. Heterozygotes were intercrossed to produce homozygous mutant mice, which were identified by Southern blot analysis of tail DNA (Figure 1B). Mating of heterozygotes yielded $Skp2^{+/+}$, $Skp2^{+/-}$ and $Skp2^{-/-}$ offspring approximately in the expected Mendelian ratio. Reverse transcriptase (RT)–PCR analysis confirmed that the $Skp2^{-/-}$ mice did not contain detectable *Skp2* mRNA (Figure 1C). Furthermore, neither full-length nor truncated Skp2 protein was detected in $Skp2^{-/-}$ cells (Figure 1D).

The body weight of the $Skp2^{-/-}$ animals was less than that of their littermate controls (approximately two-thirds of that of the wild-type littermates) (Figure 1E and F). In most instances, the homozygous mutants were the smallest animals in each litter. The mean and range of body weights

of $Skp2^{+/-}$ mice were intermediate between the corresponding values for wild-type and $Skp2^{-/-}$ mice, although there was partial overlap in the sizes of $Skp2^{+/-}$ and $Skp2^{+/+}$ animals and in those of $Skp2^{+/-}$ and $Skp2^{-/-}$ mice. These weight differences were already evident during late embryogenesis (data not shown). Despite their small size, the external proportions of $Skp2^{-/-}$ mice appeared normal. Both male and female $Skp2^{-/-}$ mice were fertile. No illness was evident in the $Skp2^{-/-}$ mice up to 10 months of age, suggesting that the absence of Skp2 does not increase the incidence of cancer, despite the abnormal accumulation of cyclin E, polyploidy and centrosome overduplication apparent in the cells of these animals (see below).

Enlargement of nuclei and polyploidy in Skp2 $^{-/-}$ mice

Necropsy revealed no gross anatomic abnormalities in $Skp2^{-/-}$ mice. However, microscopic examination revealed that the size of nuclei in $Skp2^{-/-}$ hepatocytes is markedly larger than that of nuclei in the corresponding cells of wild-type or heterozygous littermates (Figure 2A–F). Flow cytometry also demonstrated that the DNA content of hepatocytes from adult $Skp2^{-/-}$ mice ranges from 2C to 16C, whereas that of most hepatocytes from $Skp2^{+/+}$ and $Skp2^{+/-}$ animals was 2C or 4C (Figure 2G). Hepatocytes from $Skp2^{-/-}$ mice were also larger in size than those from $Skp2^{+/+}$ or $Skp2^{+/-}$ animals.

This phenotype of $Skp2^{-/-}$ cells appears to be tissue specific. Thus, similar abnormalities were observed in the lung (epithelium of bronchioles) (Figure 2H and I), kidney (epithelium of proximal renal tubules) (Figure 2J and K), embryonic fibroblasts (MEFs; see below) and testis (data not shown). The size of nuclei in cells of all other organs examined seemed to be unaffected in the mutant animals.

Reduced growth rate of and centrosome overduplication in Skp2 $^{-/-}$ cells

We prepared MEFs from $Skp2^{+/+}$, $Skp2^{+/-}$ and $Skp2^{-/-}$ embryos on embryonic day 13.5 and examined the initial growth properties of these cells in culture. At passage 2, the rate of increase in the number of $Skp2^{-/-}$ MEFs was markedly reduced compared with that for $Skp2^{+/+}$ or $Skp2^{+/-}$ MEFs (Figure 3A), whereas the rates were similar for $Skp2^{+/+}$ and $Skp2^{+/-}$ MEFs. At passage 5, $Skp2^{-/-}$ MEFs appeared to have virtually ceased proliferating, with the result that the difference in growth rate between these cells and either $Skp2^{+/+}$ or $Skp2^{+/-}$ MEFs was more pronounced. The rate of proliferation of T lymphocytes derived from $Skp2^{-/-}$ mice in response to stimulation with immobilized anti-CD3ε and anti-CD28 was also markedly reduced relative to the proliferation rate of T cells from $Skp2^{+/+}$ animals (Figure 3B). These data suggest that a reduced rate of cell growth may be a cause of the small body size of $Skp2^{-/-}$ mice. Although the cell cycle profile of $Skp2^{-/-}$ MEFs in asynchronous culture seemed almost normal, the entry of these cells into S phase appeared partially delayed, as revealed by the observation that the size of the S phase population after either γ-irradiation or release from serum deprivation was smaller for $Skp2^{-/-}$ MEFs than for $Skp2^{+/+}$ or $Skp2^{+/-}$ MEFs (data not shown).

The cell and nuclear sizes of MEFs from $Skp2^{-/-}$ mice were substantially larger than those of MEFs from wild-type animals (Figure 3C and D). Most MEFs from $Skp2^{+/+}$ or $Skp2^{+/-}$ mice contained one or two centrosomes juxtaposed to the nucleus. In contrast, $Skp2^{-/-}$ MEFs often contained more than two centrosomes (3–12 per cell) (Figure 3E–H). Quantitative analysis revealed that abnormal amplification of centrosomes during interphase was apparent in 5.2 and 5.6% of $Skp2^{+/+}$ and $Skp2^{+/-}$ MEFs, respectively, compared with a value of 38.2% for $Skp2^{-/-}$ MEFs (Figure 3I). Furthermore, micronuclei were apparent in some $Skp2^{-/-}$ MEFs (Figure 3D), possibly as a result of unbalanced segregation of chromosomes caused by the presence of multiple centrosomes. The incidence of spontaneous apoptosis among $Skp2^{-/-}$ MEFs was also about twice that among $Skp2^{+/+}$ or $Skp2^{+/-}$ MEFs (Figure 3J and K), possibly as a result of cell death triggered by the unbalanced segregation of chromosomes. Thus, the reduced growth rate of $Skp2^{-/-}$ MEFs may be attributable, at least in part, to the increased frequency of apoptosis.

Accumulation of cyclin E and p27^{Kip1} in Skp2 $^{-/-}$ cells

We examined the expression of various cell cycle regulators in MEFs from $Skp2^{+/+}$, $Skp2^{+/-}$ and $Skp2^{-/-}$ embryos. The abundance of cyclin E and $p27^{Kip1}$ was increased specifically in MEFs from $Skp2^{-/-}$ mice, whereas the amounts of cyclin A, cyclin B, CDK2 and α-tubulin were similar in the cells from all three strains of mice (Figure 4A). The accumulation of cyclin E and $p27^{Kip1}$ was also apparent in $Skp2^{-/-}$ fetal liver (Figure 4B). The amount of cyclin D1 also appeared to be slightly increased in the $Skp2^{-/-}$ MEFs; however, this increase is probably a secondary effect because Skp2 neither interacts with cyclin D1 nor promotes its ubiquitylation (see Figure 5A and B). Despite the hyperaccumulation of cyclin E in $Skp2^{-/-}$ MEFs, CDK2-associated kinase activity was not increased in these cells (Figure 4A), probably because the additional cyclin E may be free (unbound) and because the abundance of $p27^{Kip1}$, a potent inhibitor of CDK2 activity, is also increased in the mutant cells. Marti *et al*. (1999) recently showed that SCF^{Skp2} may function as a ubiquitin ligase for E2F-1, which activates the transcription of the genes for cyclins A and E, dihydrofolate reductase (DHFR) and other proteins important in DNA synthesis. However, unlike cyclin E, E2F-1 did not accumulate in $Skp2^{-/-}$ cells (Figure 4A). Consistent with this observation, the abundance of cyclin A and DHFR was also unchanged in these cells. Northern blot analysis revealed that the amount of cyclin E mRNA is not increased in $Skp2^{-/-}$ MEFs (Figure 4C). Furthermore, the half-life of cyclin E was markedly increased in $Skp2^{-/-}$ MEFs, showing directly that the rate of cyclin E proteolysis is reduced (Figure 4D). These various data suggest that Skp2 is dispensable for E2F-1 degradation, and that the accumulation of cyclin E does not result from an increase in transcription of the cyclin E gene caused by overexpression of E2F-1.

To exclude the possibility that accumulation of cyclin E is a secondary effect of inhibition of autophosphorylation by the increased abundance of $p27^{Kip1}$, we infected wild-type MEFs with a recombinant adenovirus encoding $p27^{Kip1}$. Overexpression of $p27^{Kip1}$ did not result in the accumulation of cyclin E (Figure 4E), suggesting that the

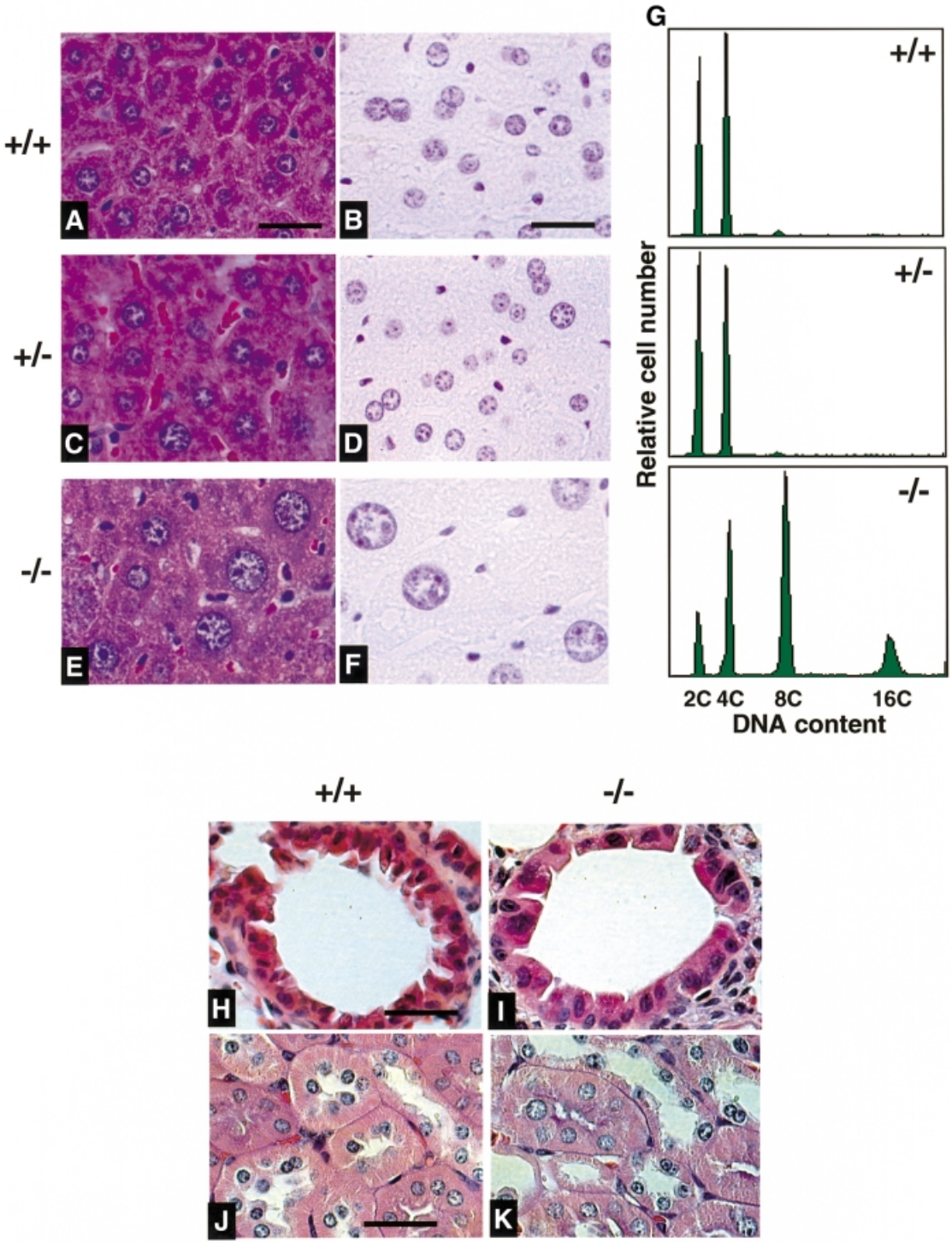

Fig. 2. Enlargement of nuclei and polyploidy in $Skp2^{-/-}$ cells. (A–F) Histological analysis of liver sections from adult $Skp2^{+/+}$ (**A** and **B**), $Skp2^{+/-}$ (**C** and **D**) and $Skp2^{-/-}$ (**E** and **F**) mice. Sections were stained with hematoxylin and eosin (A, C and E) or with Feulgen solution (B, D and F). Scale bars, 25 μm. (**G**) Flow cytometric analysis of the DNA content of hepatocytes from $Skp2^{+/+}$ (upper panel), $Skp2^{+/-}$ (middle panel) and $Skp2^{-/-}$ (bottom panel) mice. (H–K) Histological analysis of sections of bronchioles (**H** and **I**) and renal tubules (**J** and **K**) from $Skp2^{+/+}$ (H and J) and $Skp2^{-/-}$ (I and K) mice. The sections were stained with hematoxylin and eosin. Scale bars, 25 μm.

accumulation of cyclin E in $Skp2^{-/-}$ MEFs is independent of $p27^{Kip1}$ accumulation.

We next determined whether the accumulation of cyclin E and $p27^{Kip1}$ in $Skp2^{-/-}$ MEFs is reversed by infection of the cells with a recombinant adenovirus encoding Skp2. Overexpression of Skp2 in wild-type MEFs resulted in a marked decrease in the abundance of $p27^{Kip1}$ but only a small decrease in that of cyclin E (Figure 4F). This difference in the effects of Skp2 overexpression on the abundance of cyclin E and that of $p27^{Kip1}$ is consistent with previous observations (Sutterluty *et al.*, 1999), and suggests that a certain

proportion of cyclin E molecules are protected from ubiquitin-dependent proteolysis as a result of their association with CDK2. The amounts of cyclin E and $p27^{Kip1}$ in $Skp2^{-/-}$ MEFs were reduced to the levels in $Skp2^{+/+}$ MEFs, when they were infected with the adenovirus encoding Skp2, confirming that the accumulation of these two proteins in $Skp2^{-/-}$ MEFs indeed results from Skp2 deficiency, and not from an effect of abnormal expression of other genes adjacent to the *Skp2* locus.

Loss of cyclin E periodicity in $Skp2^{-/-}$ cells

We next investigated whether cyclin E is eliminated in the $Skp2^{-/-}$ cells during S–G_2 phases of the cell cycle, as occurs in normal cells. The cell cycle profiles of MEFs from $Skp2^{+/+}$ and $Skp2^{-/-}$ mice were similar at low passage numbers (data not shown). However, the amount of cyclin E remained high throughout the cell cycle in the $Skp2^{-/-}$ MEFs (Figure 4G), indicating that Skp2-mediated degradation of cyclin E is required for cyclin E periodicity during the cell cycle. This observation suggests that down-regulation of cyclin E is not obligatory for entry into S phase, in contrast to the fact that cyclin B degradation is required for exit of cells from mitosis.

Enhancement by Skp2 of ubiquitin-mediated proteolysis of cyclin E

We confirmed that, like the corresponding human proteins (Lisztwan *et al*., 1998), mouse Skp1, Cul1 and Skp2 proteins form a trimolecular SCF complex *in vivo* (data not shown). Given that cyclin E accumulated in $Skp2^{-/-}$ mice, we then investigated whether Skp2 specifically associates with cyclin E. A co-immunoprecipitation assay revealed that recombinant Skp2 interacted with cyclins A and E *in vivo* (Figure 5A). Other F-box proteins FWD1 and FWD2 did not interact with cyclins A and E (data not shown). Expression of Skp2 markedly increased the polyubiquitylation of cyclins A and E in both 293T cells (Figure 5B) and NIH 3T3 cells (data not shown). To exclude the possibility that another protein bound to cyclin E is ubiquitylated, the immunoprecipitate was boiled in SDS-containing buffer, re-immunoprecipitated and the second immunoprecipitate subjected to immunoblot analysis with anti-ubiquitin antibody. Skp2 did not interact with cyclin B or D1. Cyclin B was constitutively ubiquitylated, probably reflecting APC/C activity in cells in M–G_1 phases, regardless of the presence or absence of Skp2. Cyclin D1 ubiquitylation was not observed even in the presence of Skp2. These results indicate that Skp2 specifically targets cyclins A and E for ubiquitylation. Although it binds to cyclin A and promotes its ubiquitylation, Skp2 appears to be dispensable for cyclin A degradation in $Skp2^{-/-}$ MEFs (Figure 4A), probably because cyclin A ubiquitylation is mediated by both APC/C and SCF complexes. It is likely that the APC/C compensates in this regard for the lack of Skp2. Endogenous Skp2 was also detected by immunoblot analysis in immunoprecipitates prepared from Jurkat cell lysates with anti-cyclin E (Figure 5C), suggesting that endogenous Skp2 interacts with endogenous cyclin E under physiological conditions.

We then investigated whether Skp2 mediated ubiquitylation of cyclin E *in vitro*. Cyclin E, Skp2, Skp1 and Cul1 were expressed in and purified from insect cells infected with the corresponding recombinant baculoviruses, and the purified recombinant proteins were then incubated in various combinations together with E1, an S100 fraction of NIH 3T3 cell lysate as a source of E2 and Rbx1 (and other possible required factors), and ubiquitin. The reaction mixtures were subjected to immunoprecipitation with anti-cyclin E, and the immunoprecipitates were subjected to immunoblot analysis with anti-ubiquitin. Skp2 markedly increased the polyubiquitylation of cyclin E (Figure 5D), and this effect was enhanced further by Skp1–Cul1 (data not shown). To confirm that the ladder/smear is ubiquitylated cyclin E, we added GST-fused ubiquitin (34 kDa) instead of ubiquitin (8 kDa) to the reaction. The ladder/smear was shifted to a higher molecular weight (Figure 5D), suggesting that cyclin E is polyubiquitylated in the presence of Skp2 in the reaction. These *in vivo* and *in vitro* data thus suggested that Skp2 functions as a component of the SCF ubiquitin ligase for cyclin E.

Interaction of Skp2 with Cul1, but not with Cul3

Very recently, it has been reported that both $Cul1^{-/-}$ and $Cul3^{-/-}$ animals died *in utero* around embryonic day 6.5 and their cells exhibited accumulation of cyclin E (Dealy *et al*., 1999; Singer *et al*., 1999; Wang *et al*., 1999). Given that cells are able to tolerate high levels of cyclin E expression (Spruck *et al*., 1999) and that Skp2-deficient mice, whose cells also exhibit accumulation of cyclin E, survive the embryonic period (this study), overexpression of cyclin E may not be a direct cause of embryonic lethality in $Cul1^{-/-}$ or $Cul3^{-/-}$ mice. Because Cullin probably contributes to the ubiquitin-dependent proteolysis of numerous proteins, the early embryonic lethality in these knockout animals may be attributable to the combined effects of dysregulation of the expression of many proteins. Like Skp2, Cul3 interacts (probably indirectly) with the free (unbound), unphosphorylated form of cyclin E (Singer *et al*., 1999). However, we failed to detect an interaction between Skp2 and Cul3 *in vivo*, whereas the interaction between Skp2 and Cul1 was readily detected (Figure 5E), suggesting that Skp2 functions as the substrate recognition component in conjunction with Skp1 and Cul1, to ubiquitylate cyclin E and other proteins. The contribution of Cul3 to the ubiquitin-dependent proteolysis of cyclin E remains to be characterized in detail. In particular, the putative substrate-specific component of Cul3-based complexes remains to be identified.

Inhibition by CDK2 of the interaction between Skp2 and cyclin E

Previous data have suggested that binding of CDK2 to cyclin E protects the latter from ubiquitylation (Clurman *et al*., 1996). We therefore examined whether cyclin E complexed with CDK2 interacts with Skp2 and undergoes ubiquitylation. Co-expression of CDK2 prevented the interaction between cyclin E and Skp2 in transfected cells (data not shown) and completely inhibited the ubiquitylation of cyclin E (Figure 6A). A kinase-negative mutant of CDK2 (D145N) also inhibited both the interaction between Skp2 and cyclin E and the ubiquitylation of cyclin E, suggesting that CDK2 physically interrupts the association of Skp2 with cyclin E, rather than acting through its kinase activity. Our data thus suggested that the

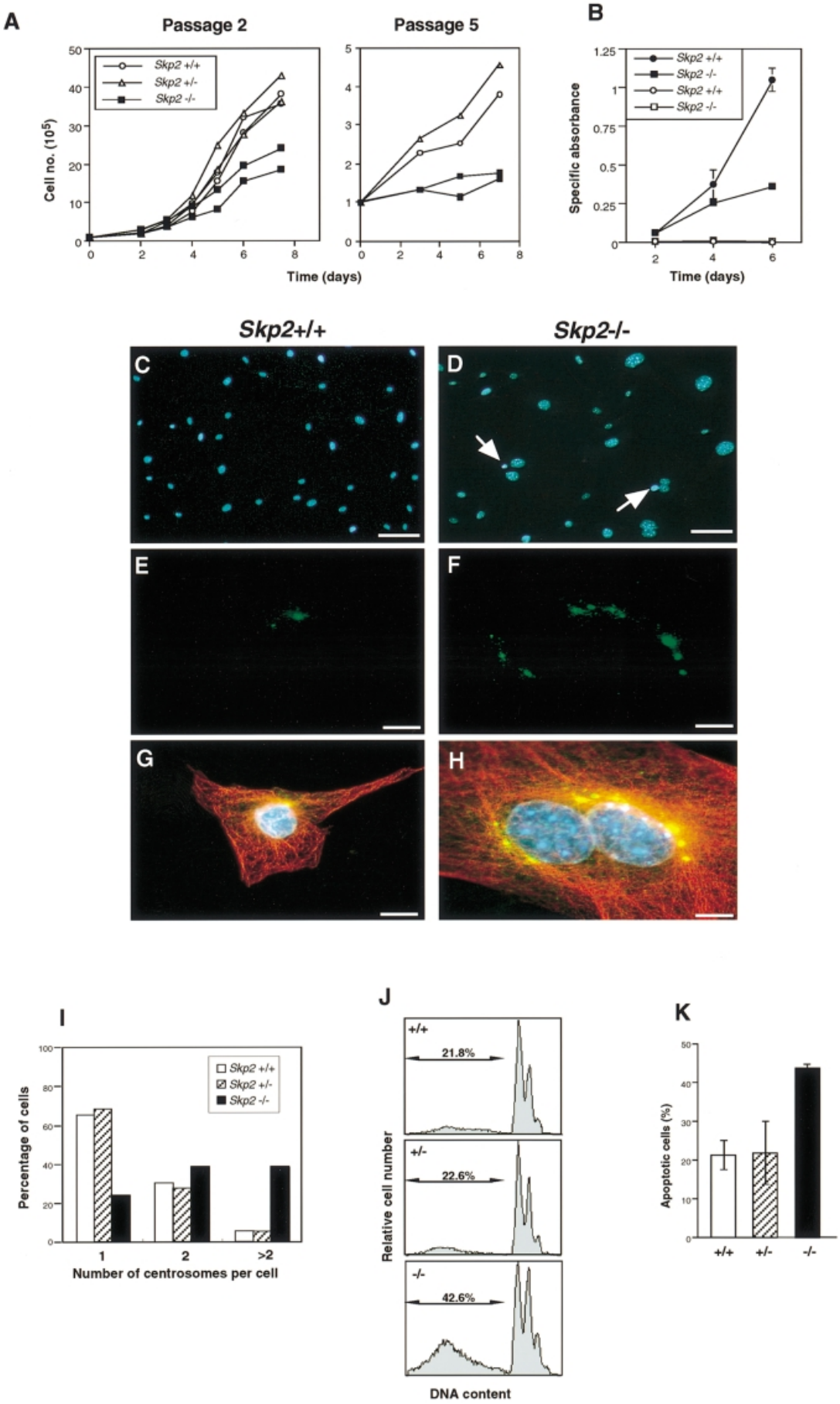
A
Passage 2
Passage 5
Skp2 +/+
Skp2 +/-
Skp2 -/-
Cell no. (10^5)
Time (days)
B
Skp2 +/+
Skp2 -/-
Skp2 +/+
Skp2 -/-
Specific absorbance
Time (days)
Skp2+/+
Skp2-/-
C
D
E
F
G
H
I
Skp2 +/+
Skp2 +/-
Skp2 -/-
Percentage of cells
Number of centrosomes per cell
J
+/+
21.8%
+/-
22.6%
-/-
42.6%
Relative cell number
DNA content
K
Apoptotic cells (%)
+/+
+/-
-/-

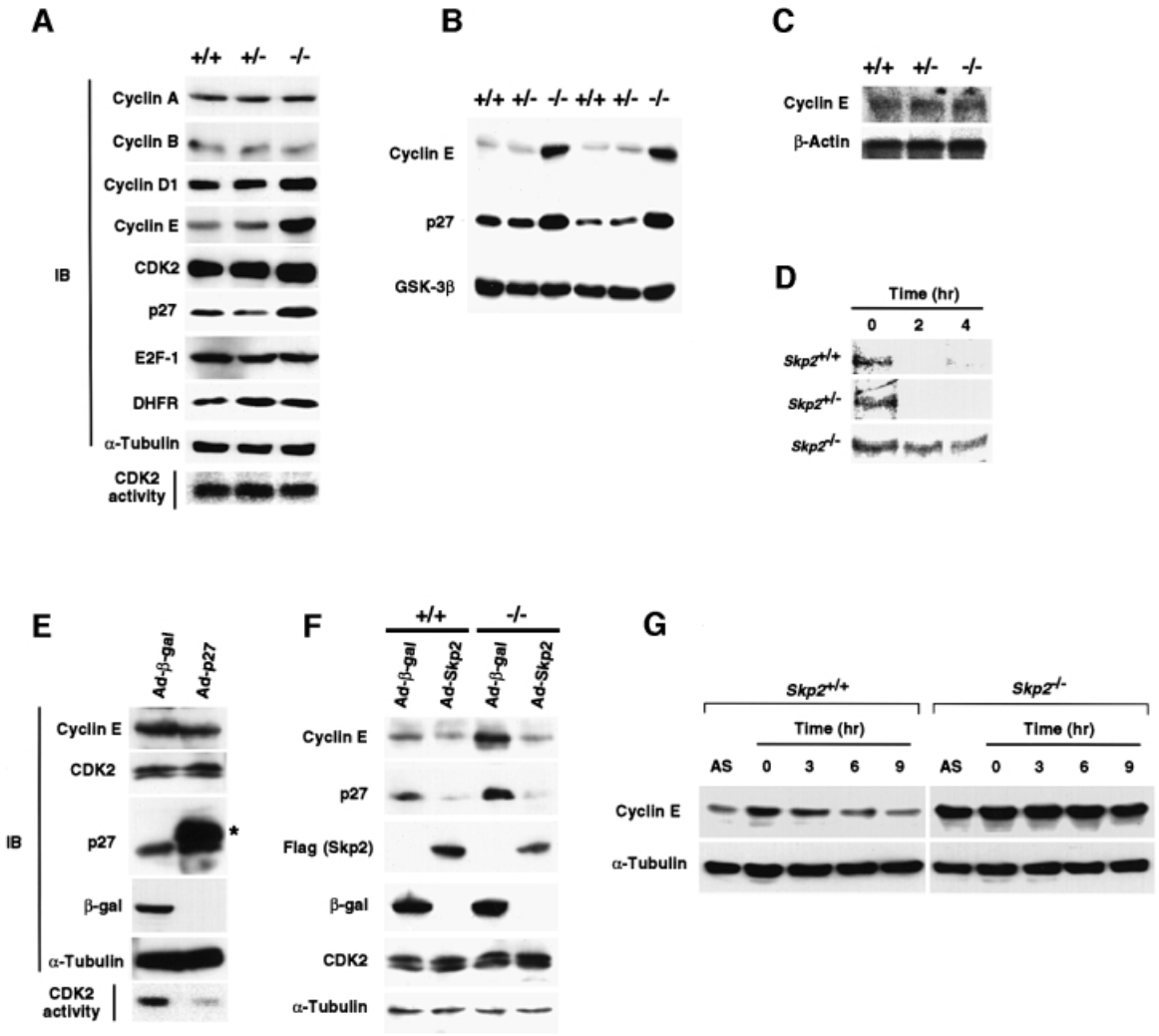

Fig. 4. Accumulation of cyclin E and loss of periodicity of cyclin E expression in $Skp2^{-/-}$ cells. (**A**) Immunoblot analysis (IB) of various cell cycle regulators in MEFs from $Skp2^{+/+}$, $Skp2^{+/-}$ and $Skp2^{-/-}$ mice. An *in vitro* assay of CDK2 kinase activity is also shown. (**B**) Abundance of cyclin E and $p27^{Kip1}$ in fetal liver from $Skp2^{+/+}$, $Skp2^{+/-}$ and $Skp2^{-/-}$ mice. Immunoblot analysis of glycogen synthase kinase-3β (GSK-3β) is also shown as a control. (**C**) Northern blot analysis of cyclin E mRNA in MEFs. Polyadenylated RNA prepared from $Skp2^{+/+}$, $Skp2^{+/-}$ and $Skp2^{-/-}$ MEFs was subjected to Northern blot analysis with mouse cyclin E cDNA or β-actin cDNA (control) probes. (**D**) Pulse–chase analysis of the turnover rate of ^{35}S-labeled cyclin E in $Skp2^{+/+}$, $Skp2^{+/-}$ and $Skp2^{-/-}$ MEFs. (**E**) Lack of effect of $p27^{Kip1}$ overexpression on the abundance of cyclin E. Wild-type MEFs were infected with recombinant adenoviral vectors encoding either β-galactosidase (Ad-β-gal) or Flag epitope-tagged $p27^{Kip1}$ (Ad-p27). Immunoblot analysis (IB) as well as an *in vitro* assay of CDK2 kinase activity were performed. The asterisk indicates the recombinant Flag-tagged $p27^{Kip1}$. (**F**) Reversed expression levels of cyclin E and $p27^{Kip1}$ by adenoviral transfer of the *Skp2* gene into $Skp2^{-/-}$ MEFs. Cells were infected with recombinant adenoviral vectors encoding β-galactosidase (Ad-β-gal) or Flag-tagged Skp2 (Ad-Skp2). Cell lysates subsequently were prepared and subjected to immunoblot analysis with antibodies to cyclin E, $p27^{Kip1}$, Flag (for Skp2), β-galactosidase, CDK2 or α-tubulin. (**G**) Impaired elimination of cyclin E during S–G_2 phases in Skp2-deficient MEFs. Cell lysates prepared from MEFs in asynchronous culture (AS) or at the indicated times after release from aphidicolin-induced cell cycle arrest were subjected to immunoblot analysis with anti-cyclin E or anti-α-tubulin (control).

Fig. 3. Reduced growth rate, abnormal amplification of centrosomes and increased incidence of apoptosis in the absence of Skp2. (**A**) Growth curves of $Skp2^{+/+}$, $Skp2^{+/-}$ and $Skp2^{-/-}$ MEFs at passage 2 (left panel) and passage 5 (right panel). Data are means of duplicate plates, and each curve corresponds to MEFs from a different animal. (**B**) Growth curves of T lymphocytes derived from $Skp2^{+/+}$ (circles) and $Skp2^{-/-}$ (squares) mice with (closed symbols) or without (open symbols) stimulation by immobilized anti-CD3ε and anti-CD28. Data are means ± SD of triplicate cultures and are expressed as specific absorbance (the absorbance value for cell cultures minus that for medium alone). (**C** and **D**) Enlargement of nuclei in $Skp2^{-/-}$ MEFs. $Skp2^{+/+}$ (C) and $Skp2^{-/-}$(D) MEFs were stained with Hoechst 33258 dye (blue) to reveal the size of nuclei. Arrows indicate the abnormal micronuclei detected specifically in $Skp2^{-/-}$ MEFs. Scale bars, 100 μm. (**E**–**H**) Overduplication of centrosomes in $Skp2^{-/-}$ MEFs. MEFs from $Skp2^{+/+}$ (E and G) and $Skp2^{-/-}$ (F and H) mice were stained with anti-pericentrin (green) either alone (E and F) or together with both anti-α-tubulin (red) and Hoechst 33258 DNA dye (blue) (G and H). Scale bars, 10 μm. (**I**) Quantitative analysis of centrosome number. Data are expressed as the percentage of cells that contained the indicated number of centrosomes. (**J**) Increased incidence of spontaneous apoptosis in $Skp2^{-/-}$ MEFs. $Skp2^{+/+}$ (top panel), $Skp2^{+/-}$ (middle panel) and $Skp2^{-/-}$ (bottom panel). MEFs at passage 2 were harvested, stained with hypotonic fluorescent solution and subjected to flow cytometry. Representative results are shown, with the percentage of hypodiploid (apoptotic) cells indicated. (**K**) Quantitative analysis of spontaneous apoptosis in MEFs. The percentage of hypodiploid cells among $Skp2^{+/+}$, $Skp2^{+/-}$ and $Skp2^{-/-}$ MEFs was determined and is expressed as the mean ± SD of values from triplicate cultures. Statistical analysis by Student's *t*-test for two independent samples yielded two-tailed *p*-values of <0.02 and <0.05 for comparison between $Skp2^{+/+}$ and $Skp2^{-/-}$ MEFs and between $Skp2^{+/-}$ and $Skp2^{-/-}$ MEFs, respectively.

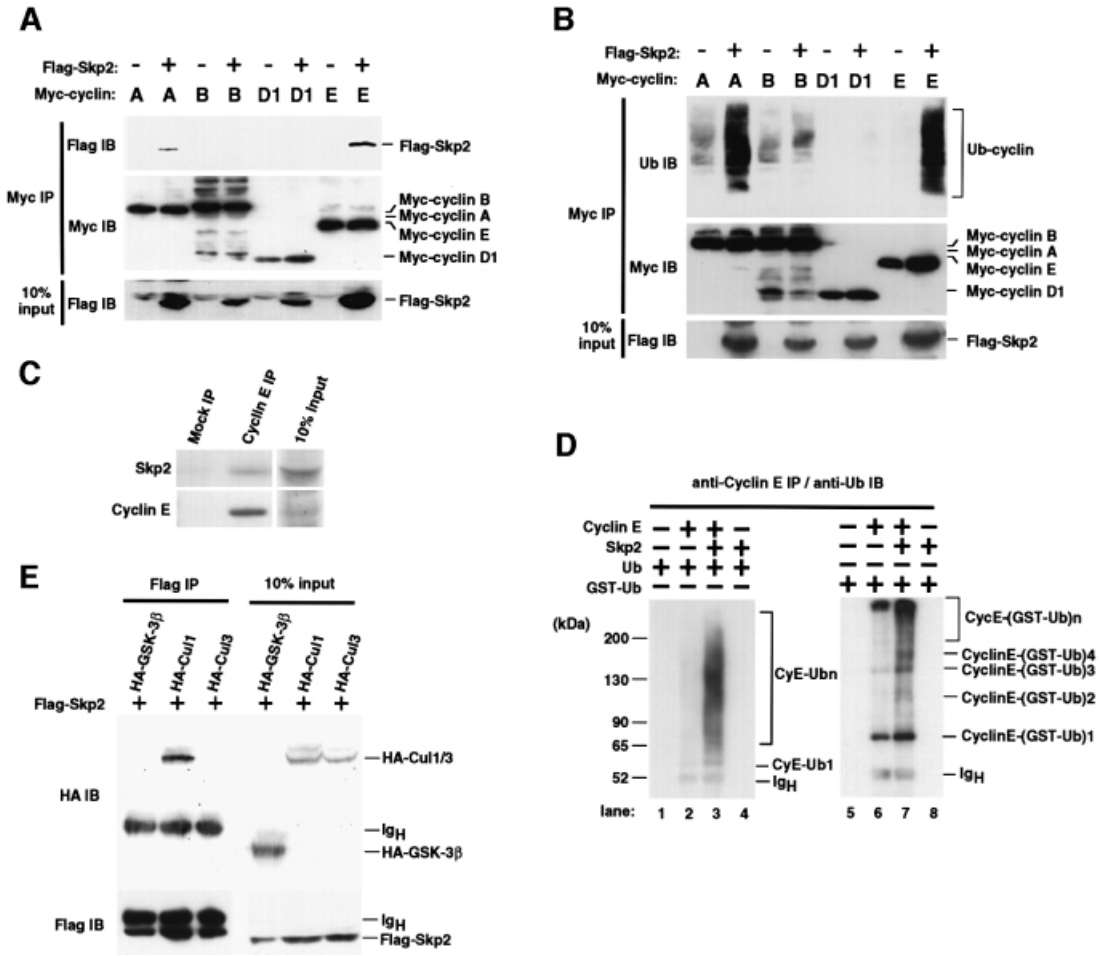

Fig. 5. Interaction of Skp2 with cyclin E and its effect on cyclin E ubiquitylation. (**A**) Binding of Skp2 to cyclins A and E. Myc-tagged cyclins A, B, D1 or E, either alone or together with Flag-Skp2, were expressed in 293T cells. Proteins immunoprecipitated with anti-Myc (Myc IP) were analyzed by immunoblotting with anti-Flag or anti-Myc. Ten percent of the input for immunoprecipitation was also subjected to immunoblot analysis with anti-Flag. (**B**) Skp2-induced ubiquitylation of cyclins A and E. Immunoprecipitates prepared as in (A) were subjected to immunoblot analysis with anti-ubiquitin or anti-Myc. (**C**) Interaction of endogenous Skp2 with endogenous cyclin E *in vivo*. Proteins immunoprecipitated from lysates of Jurkat cells with anti-cyclin E or pre-immune rabbit antibodies (mock) were subjected to immunoblotting with anti-Skp2 or anti-cyclin E. Ten percent of the input for immunoprecipitation was also subjected to immunoblotting. (**D**) Effect of Skp2 on ubiquitylation of cyclin E *in vitro*. Purified recombinant proteins were incubated in the indicated combinations together with purified E1 enzyme, an S100 fraction of NIH 3T3 cell lysate and ubiquitin. Proteins immunoprecipitated from the reaction mixtures with anti-cyclin E were analyzed by immunoblotting with anti-ubiquitin. (**E**) Skp2 was associated with Cul1, but not Cul3. HA-tagged GSK-3β (control), Cul1 or Cul3 together with Flag-Skp2 were expressed in 293T cells. Proteins immunoprecipitated with anti-Flag were analyzed by immunoblotting with anti-HA or anti-Flag. Ten percent of the input for immunoprecipitation was also subjected to immunoblotting.

binding of CDK2 to cyclin E prevents cyclin E from interacting with Skp2 and from undergoing ubiquitylation, and that cyclin E that is not complexed with CDK2 is targeted by Skp2 for ubiquitylation.

This conclusion was confirmed by an experiment with cyclin E mutants. Phosphorylation of Thr380 in cyclin E by complexed CDK2 is thought to reduce the stability of cyclin E; thus, replacement of this threonine residue with alanine (T380A) stabilizes cyclin E (Clurman *et al*., 1996; Won and Reed, 1996). However, this mutation affected neither the interaction between Skp2 and cyclin E nor the ubiquitylation of cyclin E promoted by Skp2 (Figure 6B), suggesting that phosphorylation at Thr380 may regulate cyclin E stability by a mechanism that is independent of Skp2-mediated ubiquitylation. Another cyclin E mutant, in which Arg130 is replaced by alanine (R130A), was also tested for binding to Skp2. Arg130 of cyclin E is critical for CDK2 binding, so that this mutant is unable to associate with and be phosphorylated by CDK2 (Clurman *et al*., 1996). CDK2 inhibited neither the interaction of the R130A mutant of cyclin E with Skp2 nor its basal level of ubiquitylation, which was apparent when the blot was overexposed (Figure 6B). In addition, phosphatase treatment did not induce dissociation of the Skp2–cyclin E complex, whereas it readily abolished the phosphorylation-dependent interaction between FWD1/β-TrCP and IκBα (Hatakeyama *et al*., 1999) (Figure 6C). Taken together, these observations suggest that the Skp2-induced ubiquitylation of cyclin E does not require CDK2-mediated phosphorylation. Phosphorylation of Thr187 of $p27^{Kip1}$ by the cyclin E–CDK2 complex was shown previously to be required for the interaction of this CKI

with Skp2 (Carrano *et al*., 1999). The recognition of cyclin E and $p27^{Kip1}$ by Skp2 thus appears to be achieved by distinct mechanisms.

Our data thus suggested that cyclin E that is not complexed with CDK2 is targeted by Skp2 for ubiquitylation. To investigate this hypothesis directly, we performed a sequential immunoprecipitation assay with lysates of 293T cells expressing Myc-cyclin E and Flag-Skp2. The protein complex immunoprecipitated with anti-CDK2 contained neither Skp2 nor ubiquitylated cyclin E (Figure 6D). The supernatant from this immunoprecipitation, containing Myc-cyclin E that was not complexed with CDK2, was then subjected to immunoprecipitation with anti-Myc. The resulting precipitate contained both Skp2 and ubiquitylated cyclin E, consistent both with the hypothesis that Skp2 interacts preferentially with free cyclin E and thereby promotes its ubiquitylation, and with the previous observation that free cyclin E is targeted for ubiquitylation. A pulse–chase experiment revealed that Skp2 markedly increased the turnover rate of cyclin E (Figure 6E). Consistent with our binding and ubiquitylation data, co-expression of CDK2 with Skp2 prevented the stimulatory effect of the latter on cyclin E degradation.

Discussion

Protein degradation by the ubiquitin–proteasome pathway plays a fundamental role in determining the abundance of important regulatory proteins. Although ubiquitin ligases are thought to determine substrate specificity in this pathway, specific targets have been identified for few such E3 enzymes in higher eukaryotes. The mammalian F-box protein Skp2 was isolated originally as a molecule that binds to cyclin A–CDK2 (Zhang *et al*., 1995). More recently, Skp2 was shown to participate in the ubiquitylation of the CKI $p27^{Kip1}$ and the transcription factor E2F-1 (Carrano *et al*., 1999; Marti *et al*., 1999; Tsvetkov *et al*., 1999). Our present data show that Skp2 interacts with cyclin E and thereby induces its ubiquitin-dependent proteolysis, and that cells that lack Skp2 accumulate both cyclin E and $p27^{Kip1}$ as a result of a specific impairment in the degradation of these proteins. These observations provide, as far as we are aware, the first genetic evidence that an F-box protein plays a physiological role in the degradation of a specific protein substrate in mammals. Our results thus suggest that SCF^{Skp2} is a bona fide ubiquitin ligase for both cyclin E and $p27^{Kip1}$.

Although the precise mechanisms responsible for monitoring centrosome number and function are unknown, recent studies with cell-free assays have suggested that cyclin E-dependent kinase activity is required for centrosome duplication (Hinchcliffe *et al*., 1999). Permanent centrosome duplication is observed during early embryogenesis, in which, as in $Skp2^{-/-}$ cells, cyclin E is not degraded periodically (Hinchcliffe *et al*., 1999; Karsenti, 1999). Thus, the overduplication of centrosomes apparent in $Skp2^{-/-}$ cells is likely to be attributable to the overexpression and retention of cyclin E. Meraldi *et al*. (1999) showed that the kinase that appears to be directly responsible for the initiation of centrosome duplication may not be cyclin E–CDK2 but rather cyclin A–CDK2, as well as E2F transcription factors in somatic cells. However, neither cyclin A nor E2F-1 accumulates in $Skp2^{-/-}$ cells, suggesting that overexpression of cyclin E is the more likely cause of centrosome overduplication in these cells. However, total CDK2 activity was not altered in $Skp2^{-/-}$ cells. One possible explanation for this apparent discrepancy is that both positive and negative regulators of the cell cycle accumulate in $Skp2^{-/-}$ cells, but that the precise timing of the activation and the localization of these regulators may be altered in $Skp2^{-/-}$ cells, resulting in defects in maintenance of the numbers of chromosomes and centrosomes. These possibilities remain to be tested in the future. It also remains possible that other unidentified substrates that suppress centrosome duplication may be targeted by SCF^{Skp2}. Skp1 and Cul1, both components of the SCF ubiquitin ligase, have been shown to localize to the centrosome (Freed *et al*., 1999; Gstaiger *et al*., 1999), suggesting that Skp2 might mediate ubiquitylation of substrates in the centrosome. Transient transfection experiments indicate that Skp2 is localized predominantly in the nucleus but is also present in the cytoplasm (Miura *et al*., 1999). Although focal expression of Skp2 at the centrosome was not detected in this previous study, it remains possible that this protein is localized at this site.

It is of note that a mutant fission yeast lacking the F-box protein Pop1 exhibits polyploidy (Kominami and Toda, 1997). In a *pop1* mutant, the CDK inhibitor Rum1 and the S-phase regulator Cdc18 accumulate to high levels. In fission yeast, maintenance of genome ploidy is controlled by at least two mechanisms: Cdc2/Cdc13 (B-type cyclin) and Cdc18. Thus, it is highly likely that the inhibition of Cdc2/Cdc13 kinase activity by overexpression of Rum1 results in polyploidization due to bypass of M phase in the mutant (Correa-Bordes and Nurse, 1995). Similarly, the successive S phase driven by overexpression of Cdc18 may also be involved in the polyploidization (Nishitani and Nurse, 1995). Given the similarities of the mutant phenotypes of Pop1 and Skp2, accumulation of $p27^{Kip1}$ and cyclin E in $Skp2^{-/-}$ cells may correspond functionally to that of Rum1 and Cdc18 in the *pop1* mutant. Thus we are generating double-mutant mice lacking both *Skp2* and *p27* genes to examine whether the accumulation of $p27^{Kip1}$ is essential for the polyploidy and centrosome overduplication.

The abnormally high number of centrosomes present in many human tumor cell types may lead directly to aneuploidy and genomic instability through the formation of multipolar mitotic spindles. In addition, cyclin E overexpression can result in genomic instability and increase the percentage of cells exhibiting polyploidy (Spruck *et al*., 1999). Indeed, dysregulation of cyclin E is apparent in many types of neoplasm (Keyomarsi and Herliczek, 1997), suggesting that mutations in *Skp2* might contribute to such dysregulation. Furthermore, the human *Skp2* gene is located on chromosome 5p13, near a site of frequent deletion in lung carcinomas (Demetrick *et al*., 1996). These various observations support the notion that the loss of Skp2 might lead to carcinogenesis. However, given that $Skp2^{-/-}$ mice do not appear to exhibit a predisposition to cancer, the loss of Skp2 *per se* does not seem to result directly in carcinogenesis, despite the polyploidy and multiple centrosomes apparent in $Skp2^{-/-}$ cells. It is possible that the accumulation of $p27^{Kip1}$ in $Skp2^{-/-}$ cells counteracts, at least in part, the growth-promoting effect of cyclin E-dependent kinase activity.

Our data with *Skp2*$^{-/-}$ mice also suggest that mechanisms other than those that underlie chromosome and centrosome instability might contribute to tumorigenesis. Thus, cell cycle checkpoints or susceptibility to apoptosis, both of which appear normal in *Skp2*$^{-/-}$ mice (data not shown), might play an important role in tumorigenesis. The

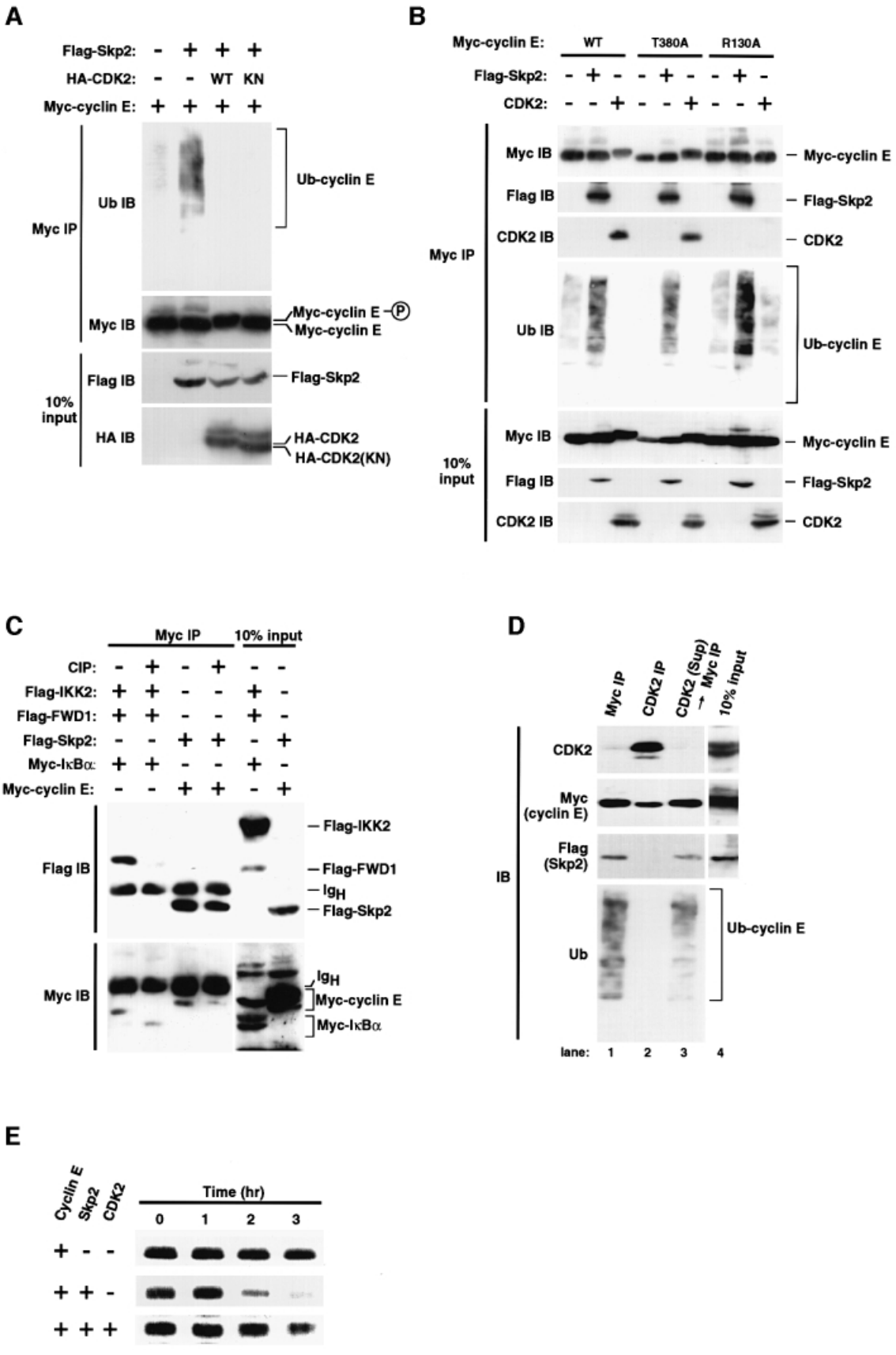

possibility remains, however, that the loss of Skp2 might be a critical step in the development of certain human cancers.

Materials and methods

Construction of Skp2 targeting vector and generation of *Skp2*$^{-/-}$ mice

Cloned genomic DNA corresponding to the Skp2 locus was isolated from a 129/Sv mouse genomic library (Stratagene). The targeting vector, pSKP2.KO, was constructed by replacing a 13 kb *Sma*I–*Sac*II fragment containing exons 1–4 with a PGK-neo-poly(A) cassette. The targeting vector thus contained 1.1 and 7.5 kb regions of homology 5′ and 3′ of the neomycin resistance marker, respectively. The PGK-tk-poly(A) cassette was ligated at the 3′ end of the insert. The maintenance, transfection and selection of ES cells were performed as described (Nakayama *et al*., 1996). The recombination event was confirmed by Southern blot analysis with the 0.7 kb *Acc*I–*Spe*I probe that flanked the 5′ homology region (Figure 1A). The expected sizes of hybridizing fragments by *Pst*I digestion are 5.3 and 4.8 kb for wild-type and mutant *Skp2* alleles, respectively.

The mutant ES cells were microinjected into C57BL/6 blastocysts, and the resulting male chimeras were mated with female C57BL/6 mice. The germline transmission of injected ES cells was confirmed by Southern blot analysis under the same conditions as above. Heterozygous offspring were intercrossed to produce homozygous mutant animals. Whole-cell lysates of MEFs were subjected to RT–PCR as described (Nakayama *et al*., 1993) with F1 (5′-CAAGCATTCAAAACTCCTGAA-3′) and F2 (5′-CACAGTCACGTCTGGGTGCAGATT-3′) primers to confirm the deletion of *Skp2*. RT–PCR analysis of β-tubulin mRNA was also performed as a control with β1 (5′-TCACTGTGCCTGAACTTACC-3′) and β2 (5′-GGAACATAGCCGTAAACTGC-3′) primers. All mice were maintained in a specific pathogen-free animal facility at the Medical Institute of Bioregulation, Kyushu University.

Histology

Tissues were dissected, fixed in 10% buffered formaldehyde and embedded in paraffin. Sections (3 μm thick) were prepared and stained with hematoxylin and eosin. The Feulgen reaction was initiated, after removal of paraffin, by incubation of the sections in 1 M HCl for 10 min at 60°C. The sections were subsequently incubated in Schiff solution for 30 min at room temperature. After three 5 min washes with 0.5% sodium hydrogen sulfate, sections were washed with tap water for 3 min and mounted on slides for microscopic analysis.

Preparation of MEFs

Primary MEFs were obtained from embryos on embryonic day 13.5 and cultured as previously described (Nakayama *et al*., 1996). For growth rate analysis, the cells were plated in 10 cm culture dishes at a density of 1×10^5 cells per dish. For cell synchronization and cell cycle analysis, MEFs were arrested at the G_1–S boundary by culture in the presence of aphidicolin (1 μg/ml) for 14 h. The cells were released from aphidicolin block by washing with and culture for various times in aphidicolin-free medium. At the indicated times, cells were harvested and either subjected to cell cycle analysis or lysed for immunoblot analysis as described below.

Flow cytometry

Suspensions of single hepatocyte nuclei for determination of DNA content were prepared from liver as described previously (Weeda *et al*., 1997). For detection of apoptosis, MEFs were harvested and stained with hypotonic fluorescent solution (Nicoletti *et al*., 1991). All analyses were performed with a FACSCalibur flow cytometer and Cell Quest software (Becton Dickinson).

Immunofluorescence microscopy

Immunocytochemical analysis of centrosomes and microtubules was performed as described (Zhou *et al*., 1998) with some modifications. Centrosomes and microtubules were stained with rabbit anti-pericentrin (PRB-432C; Corance) and mouse anti-α-tubulin (TU-01; Zymed), respectively, and immune complexes were detected with Alexa488-conjugated goat anti-rabbit immunoglobulin G (IgG) (green; Molecular Probes) and Alexa546-conjugated goat anti-mouse IgG (red; Molecular Probes), respectively. Nuclei were stained with Hoechst 33258 dye (blue).

Lymphocyte proliferation assay

Single-cell suspensions were prepared from lymph nodes of 4-month-old mice. Lymphocytes (1×10^4) were transferred to the wells of 96-well plates that had been coated with anti-CD3ε and anti-CD28 (PharMingen). Proliferation was monitored after 48, 96 or 144 h of culture with the use of an XTT colorimetric assay (Boehringer Mannheim). Absorbance at 490 nm, which correlates with viable cell number, was measured with a Benchmark microplate reader (Bio-Rad).

Construction of expression plasmids and mutagenesis

Complementary DNAs encoding mouse Skp2, FWD1 and IKK2 tagged at their N-termini with the Flag epitope, as well as those encoding human cyclins A, B, D1 or E and mouse IκBα tagged at their N-termini with the Myc epitope, or human CDK2 tagged at its N-terminus with the HA epitope, were generated by PCR with the high-fidelity, thermostable DNA polymerase KOD (Toyobo), sequenced, and subcloned into pcDNA3 (Invitrogen). The pcDNA3 vectors encoding the Myc-cyclin E substitution mutants R130A or T380A or the CDK2 substitution mutant D145N were generated with the use of a QuickChange site-directed mutagenesis kit (Stratagene).

Recombinant adenovirus generation and infection

Complementary DNAs encoding $p27^{Kip1}$ and Skp2 tagged at their N-termini with the Flag epitope, as well as those encoding β-galactosidase, were inserted at the *Swa*I site in pAxCAwt cosmid vector (Takara). Recombinant viruses were generated by co-transfecting the recombinant cosmid DNA, and Ad5-dlX adenovirus DNA digested previously with *Eco*T22I, into 293 cells according to the manufacturer's protocol (Takara). Recombinant adenoviruses were selected by serial re-infection

Fig. 6. Targeting of free cyclin E for Skp2-mediated ubiquitylation. (**A**) Effect of CDK2 on Skp2-mediated cyclin E ubiquitylation *in vivo*. Myc-tagged cyclin E either alone or together with Flag-tagged Skp2, HA-tagged wild-type (WT) CDK2 or an HA-tagged kinase-negative mutant (KN) of CDK2 were expressed in 293T cells. Proteins immunoprecipitated with anti-Myc were analyzed by immunoblotting with anti-Flag or anti-HA. Ten percent of the input for immunoprecipitation was also subjected to immunoblotting. (**B**) Interaction of the cyclin E mutants T380A and R130A with Skp2 and the effects of CDK2 on their ubiquitylation. Myc-tagged wild-type (WT) or mutant (T380A or R130A) cyclin E, Flag-Skp2 and HA-CDK2 were expressed in 293T cells. Proteins immunoprecipitated with anti-Myc were analyzed by immunoblotting with anti-Myc, anti-Flag, anti-CDK2 or anti-ubiquitin (this figure is overexposed compared with the others to show the basal level of cyclin E ubiquitylation). Ten percent of the input for immunoprecipitation was also subjected to immunoblotting. (**C**) Effect of phosphatase treatment on FWD1–IκBα and Skp2–cyclin E complexes. Myc-cyclin E, Myc-IκBα, Flag-Skp2, Flag-FWD1 and Flag-IKK2 (IκB kinase 2) were expressed in 293T cells. Proteins immunoprecipitated with anti-Myc were subjected (or not) to phosphatase (CIP) treatment and then to immunoblot analysis with anti-Flag or anti-Myc. Ten percent of the input for immunoprecipitation was also subjected to immunoblot analysis. (**D**) Sequential immunoprecipitation assay showing that only free cyclin E associates with Skp2 and undergoes ubiquitylation. 293T cells were transfected with expression plasmids encoding Myc-cyclin E and Flag-Skp2. Cell lysates were subjected to immunoprecipitation with anti-Myc (lane 1) or with anti-CDK2 (lane 2), and the resulting immunoprecipitates were subjected to immunoblot analysis with anti-CDK2, anti-Myc, anti-Flag or anti-ubiquitin. Cyclin E remaining in the supernatant (Sup) after immunoprecipitation with anti-CDK2 was then immunoprecipitated with anti-Myc and subjected to immunoblot analysis (lane 3). A portion of the cell lysate corresponding to 10% of the input for immunoprecipitation was also subjected to immunoblot analysis with anti-CDK2, anti-Myc or anti-Flag (lane 4). (**E**) Pulse–chase analysis of the effects of Skp2 and CDK2 on the turnover rate of cyclin E. Myc-cyclin E, Flag-Skp2 and CDK2 were expressed and radiolabeled in 293T cells. After incubation for the indicated times in the absence of isotope, radiolabeled proteins immunoprecipitated with the anti-Myc were analyzed by SDS–PAGE and autoradiography.

of 293 cells and finally amplified in 293 cells, and stored at –80°C. MEFs were used at passage 2, and were infected with the indicated recombinant adenovirus for 48 h.

Transfection, immunoprecipitation and immunoblot analysis

Transfection, immunoprecipitation and immunoblot analysis were performed as described (Hatakeyama *et al*., 1999). For detection of ubiquitylated proteins, after extensive washing with lysis buffer the immunoprecipitates were boiled for 5 min with RIPA buffer [10 mM Tris–HCl pH 7.4, 150 mM NaCl, 1% (v/v) NP-40, 0.1% (w/v) sodium deoxycholate, 0.1% SDS, 1 mM EDTA, 10 mM NaF, 10 mM sodium pyrophosphate]; the supernatants were then again subjected to immunoprecipitation for 4 h at 4°C with 5 μg of the required antibodies and protein G–Sepharose beads.

To detect the expression of cyclins and other proteins in MEFs, we subjected equal amounts of cell lysate protein (100 μg) to immunoblot analysis with antibodies to cyclin A (H-432; Santa Cruz), cyclin B (GNS-1; PharMingen), cyclin D1 (MBL), cyclin E (M-20; Santa Cruz), CDK2 (M2; Santa Cruz), α-tubulin (TU-01; Zymed), E2F-1 (43; Transduction Laboratories), DHFR (49; Transduction Laboratories), $p27^{Kip1}$ (57; Transduction Laboratories), GSK-3β (7; Transduction Laboratories) or β-galactosidase (clone 200-193; Oncogene Research Products).

For calf intestinal alkaline phosphatase (CIP) treatment, immunoprecipitates were equilibrated with 100 μl of a solution containing 50 mM Tris–HCl pH 8.5 and 0.1 mM EDTA, and were then incubated for 24 h at 37°C with 100 U of CIP (Roche). After extensive washing with lysis buffer, the immunoprecipitates were subjected to immunoblot analysis with anti-Flag or anti-Myc (1 μg/ml).

CDK2-associated kinase activity was assessed with an immune complex kinase assay as described (Nakayama *et al*., 1996).

In vitro assay of ubiquitylation

Complementary DNAs encoding GST fusion proteins of cyclin E, Skp2, FWD1, Skp1 or Cul1 were introduced into pBacPAK9, and the resulting vectors were used to transfect Sf9 insect cells and thereby to obtain recombinant baculoviruses. Sf9 cells were infected with the resulting viruses, and the encoded GST fusion proteins were purified from cell lysates with the use of glutathione beads. The GST sequence was cleaved from the purified fusion proteins with PreScission protease (Amersham Pharmacia Biotech). The reaction conditions are described elsewhere (Hatakeyama *et al*., 1999).

Pulse–chase experiments

Transfected 293T cells or MEFs were metabolically labeled with Trans-^{35}S (ICN) at a concentration of 100 μCi/ml for 1 h, and were then incubated for various times in the absence of isotope. Cell lysates were subjected to immunoprecipitation with anti-Myc or anti-cyclin E (M-20; Santa Cruz), and the resulting precipitates were subjected to SDS–PAGE, autoradiography and image analysis (BAS-2000; Fuji Film).

Northern blot analysis

Total RNA was isolated from MEFs with an Isogen RNA preparation kit (Nippon Gene). Polyadenylated RNA was purified from the total RNA with Oligotex-dT30 Super beads (Takara Biomedicals), subjected (1 μg) to electrophoresis on a 1% agarose gel containing 5.5% formaldehyde and transferred to a nylon membrane (Biodyne B; Pall). The blot was then subjected to hybridization with ^{32}P-labeled full-length mouse cyclin E cDNA as a probe; it was subsequently reprobed with ^{32}P-labeled β-actin cDNA after stripping of the cyclin E probe in 0.5% SDS at 100°C. Hybridization was performed at 42°C in Ultrahyb solution (Ambion) under the recommended conditions.

GenBank accession number

The accession number for the nucleotide and predicted amino acid sequences of mouse *Skp2* is AF083215.

Acknowledgements

We thank H.Sawa for the recombinant adenovirus encoding $p27^{Kip1}$; K.Kominami, N.Watanabe and M.Ohtsubo for helpful discussions; Y.Yamada, K.Shimoharada, S.Matsushita, N.Nishimura, R.Yasukochi, M.Miura, A.Yamanaka and other laboratory members for technical assistance; and M.Kimura for secretarial assistance. This work was supported in part by a grant from the Ministry of Education, Science, Sports, and Culture of Japan.

References

Bai,C., Sen,P., Hofmann,K., Ma,L., Goebl,M., Harper,J.W. and Elledge,S.J. (1996) SKP1 connects cell cycle regulators to the ubiquitin proteolysis machinery through a novel motif, the F-box. *Cell*, **86**, 263–274.

Carrano,A.C., Eytan,E., Hershko,A. and Pagano,M. (1999) SKP2 is required for ubiquitin-mediated degradation of the CDK inhibitor p27. *Nature Cell Biol.*, **1**, 193–199.

Clurman,B.E., Sheaff,R.J., Thress,K., Groudine,M. and Roberts,J.M. (1996) Turnover of cyclin E by the ubiquitin–proteasome pathway is regulated by cdk2 binding and cyclin phosphorylation. *Genes Dev.*, **10**, 1979–1990.

Correa-Bordes,J. and Nurse,P. (1995) $p25^{Rum1}$ orders S phase and mitosis by acting as an inhibitor of the $p34^{cdc2}$ mitotic kinase. *Cell*, **83**, 1001–1009.

Dealy,M., Nguyen,K.V.T., Lo,J., Gstaiger,M., Krek,W., Elson,D., Arbeit,J., Kipreos,E.T. and Johnson,R.S. (1999) Loss of Cul1 results in early embryonic lethality and dysregulation of cyclin E. *Nature Genet.*, **23**, 245–248.

Demetrick,D.J., Zhang,H. and Beach,D.H. (1996) Chromosomal mapping of the genes for the human CDK2/cyclin A-associated proteins p19 (SKP1A and SKP1B) and p45 (SKP2). *Cytogenet. Cell. Genet.*, **73**, 104–107.

Feldman,R.M., Correll,C.C., Kaplan,K.B. and Deshaies,R.J. (1997) A complex of Cdc4p, Skp1p and Cdc53p/cullin catalyzes ubiquitination of the phosphorylated CDK inhibitor Sic1p. *Cell*, **91**, 221–230.

Freed,E., Lacey,K.R., Huie,P., Lyapina,S.A., Deshaies,R.J., Stearns,T. and Jackson,P.K. (1999) Components of an SCF ubiquitin ligase localize to the centrosome and regulate the centrosome duplication cycle. *Genes Dev.*, **13**, 2242–2257.

Gstaiger,M., Marti,A. and Krek,W. (1999) Association of human SCF (SKP2) subunit p19 (SKP1) with interphase centrosomes and mitotic spindle poles. *Exp. Cell Res.*, **247**, 554–562.

Hatakeyama,S. *et al*. (1999) Ubiquitin-dependent degradation of IκBα is mediated by a ubiquitin ligase Skp1/Cul1/F-box protein FWD1. *Proc. Natl Acad. Sci. USA*, **96**, 3859–3863.

Hershko,A. and Ciechanover,A. (1998) The ubiquitin system. *Annu. Rev. Biochem.*, **67**, 425–479.

Hershko,A., Heller,H., Elias,S. and Ciechanover,A. (1983) Components of ubiquitin–protein ligase system. Resolution, affinity purification and role in protein breakdown. *J. Biol. Chem.*, **258**, 8206–8214.

Hinchcliffe,E.H., Li,C., Thompson,E.A., Maller,J.L. and Sluder,G. (1999) Requirement of Cdk2–cyclin E activity for repeated centrosome reproduction in *Xenopus* egg extracts. *Science*, **283**, 851–854.

Karsenti,E. (1999) Centrioles reveal their secrets. *Nature Cell Biol.*, **1**, E62–E64.

Keyomarsi,K. and Herliczek,T.W. (1997) The role of cyclin E in cell proliferation, development and cancer. *Prog. Cell Cycle Res.*, **3**, 171–191.

King,R.W., Peters,J.M., Tugendreich,S., Rolfe,M., Hieter,P. and Kirschner,M.W. (1995) A 20S complex containing CDC27 and CDC16 catalyzes the mitosis-specific conjugation of ubiquitin to cyclin B. *Cell*, **81**, 279–288.

Kominami,K. and Toda,T. (1997) Fission yeast WD-repeat protein Pop1 regulates genome ploidy through ubiquitin–proteasome-mediated degradation of the CDK inhibitor Rum1 and the S-phase initiator Cdc18. *Genes Dev.*, **11**, 1548–1560.

Lisztwan,J., Marti,A., Sutterluty,H., Gstaiger,M., Wirbelauer,C. and Krek,W. (1998) Association of human CUL-1 and ubiquitin-conjugating enzyme CDC34 with the F-box protein $p45^{SKP2}$: evidence for evolutionary conservation in the subunit composition of the CDC34–SCF pathway. *EMBO J.*, **17**, 368–383.

Marti,A., Wirbelauer,C., Scheffner,M. and Krek,W. (1999) Interaction between the ubiquitin–protein ligase SCF^{SKP2} and E2F-1 underlies the regulation of E2F-1 degradation. *Nature Cell Biol.*, **1**, 14–19.

Meraldi,P., Lukas,J., Fry,A.M., Bartek,J. and Nigg,E.A. (1999) Centrosome duplication in mammalian somatic cells requires E2F and Cdk2–cyclin A. *Nature Cell Biol.*, **1**, 88–93.

Miura,M., Hatakeyama,S., Hattori,K. and Nakayama,K.-i. (1999) Structure and expression of the gene encoding mouse F-box protein, Fwd2. *Genomics*, **62**, 50–58.

Nakayama,K., Ishida,N., Shirane,M., Inomata,A., Inoue,T., Shishido,N., Horii,I., Loh,D.Y. and Nakayama,K.-i. (1996) Mice lacking $p27^{Kip1}$

display increased body size, multiple organ hyperplasia, retinal dysplasia and pituitary tumors. *Cell*, **85**, 707–720.

Nakayama,K.-i. *et al*. (1993) Disappearance of the lymphoid system in Bcl-2 homozygous mutant chimeric mice. *Science*, **261**, 1584–1588.

Nicoletti,I., Migliorati,G., Pagliacci,M.C., Grignani,F. and Riccardi,C. (1991) A rapid and simple method for measuring thymocyte apoptosis by propidium iodide staining and flow cytometry. *J. Immunol. Methods*, **139**, 271–279.

Nishitani,H. and Nurse,P. (1995) p65Cdc18 plays a major role controlling the initiation of DNA replication in fission yeast. *Cell*, **83**, 397–405.

Pagano,M., Tam,S.W., Theodoras,A.M., Beer-Romero,P., Del Sal,G., Chau,V., Yew,P.R., Draetta,G.F. and Rolfe,M. (1995) Role of the ubiquitin–proteasome pathway in regulating abundance of the cyclin-dependent kinase inhibitor p27. *Science*, **269**, 682–685.

Scheffner,M., Nuber,U. and Huibregtse,J.M. (1995) Protein ubiquitination involving an E1–E2–E3 enzyme ubiquitin thioester cascade. *Nature*, **373**, 81–83.

Singer,J.D., Gurian-West,M., Clurman,B. and Roberts,J.M. (1999) Cullin-3 targets cyclin E for ubiquitination and control of S phase in mammalian cells. *Genes Dev.*, **13**, 2375–2387.

Skowyra,D., Craig,K.L., Tyers,M., Elledge,S.J. and Harper,J.W. (1997) F-box proteins are receptors that recruit phosphorylated substrates to the SCF ubiquitin–ligase complex. *Cell*, **91**, 209–219.

Spruck,C.H., Won,K.A. and Reed,S.I. (1999) Deregulated cyclin E induces chromosome instability. *Nature*, **401**, 297–300.

Sudakin,V., Ganoth,D., Dahan,A., Heller,H., Hershko,J., Luca,F.C., Ruderman,J.V. and Hershko,A. (1995) The cyclosome, a large complex containing cyclin-selective ubiquitin ligase activity, targets cyclins for destruction at the end of mitosis. *Mol. Biol. Cell*, **6**, 185–197.

Sutterluty,H., Chatelain,E., Marti,A., Wirbelauer,C., Senften,M., Muller,U. and Krek,W. (1999) $p45^{Skp2}$ promotes $p27^{Kip1}$ degradation and induces S phase in quiescent cells. *Nature Cell Biol.*, **1**, 207–214.

Tsvetkov,L.M., Yeh,K.H., Lee,S.J., Sun,H. and Zhang,H. (1999) $p27^{Kip1}$ ubiquitination and degradation is regulated by the SCF^{Skp2} complex through phosphorylated Thr187 in p27. *Curr. Biol.*, **9**, 661–664.

Wang,Y., Penfold,S., Tang,X., Hattori,N., Riley,P., Harper,J.W., Cross,J.C. and Tyers,M. (1999) Deletion of the *Cul1* gene in mice causes arrest in early embryogenesis and accumulation of cyclin E. *Curr. Biol.*, **9**, 1191–1194.

Weeda,G. *et al*. (1997) Disruption of mouse ERCC1 results in a novel repair syndrome with growth failure, nuclear abnormalities and senescence. *Curr. Biol.*, **7**, 427–439.

Weissman,A.M. (1997) Regulating protein degradation by ubiquitination. *Immunol. Today*, **18**, 189–198.

Won,K.A. and Reed,S.I. (1996) Activation of cyclin E/CDK2 is coupled to site-specific autophosphorylation and ubiquitin-dependent degradation of cyclin E. *EMBO J.*, **15**, 4182–4193.

Zachariae,W. and Nathmyth,K. (1999) Whose end is destruction: cell division and the anaphase-promoting complex. *Genes Dev.*, **13**, 2039–2058.

Zhang,H., Kobayashi,R., Galaktionov,K. and Beach,D. (1995) p19Skp1 and p45Skp2 are essential elements of the cyclin A–CDK2 S phase kinase. *Cell*, **82**, 915–925.

Zhou,H., Kuang,J., Zhong,L., Kuo,W.L., Gray,J.W., Sahin,A., Brinkley,B.R. and Sen,S. (1998) Tumour amplified kinase STK15/BTAK induces centrosome amplification, aneuploidy and transformation. *Nature Genet.*, **20**, 189–193.

Received February 21, 2000; revised and accepted March 8, 2000